

## **CHAPTER 7**

### **SURFACE EXPOSURE DATING**

Landscape of a region is a product of interaction between various geo-environmental factors like tectonics, time, climate, structure and lithology (Bloom,1998; Miliarisis and Iliopoulou, 2004; Kuhni and Pfiffner, 2001; Chorley et al., 1984; Morisawa, 1985). Therefore, information on all these factors are very much essential for developing an effective landscape evolutionary model of the terrain. In landscape evolutionary studies, timing of an event or time since the formation of a landscape is also an important aspect. The previous chapters were dealt with the morphology, tectonic and lithological characteristics of the fault scarps along the KMF. A microlevel scanning of literature reveals that no attempt has so far been made to establish the timing of scarp evolution along the KMF in the KRB. Therefore, an attempt has been made in this chapter to address the timing of scarp forming events along the KMF using surface exposure dating. The cosmogenic nuclides and exposure dating have gained importance in dating geomorphic landforms and surfaces in the last few decades. The present chapter dealt with dating of bedrock fault scarps and selected landforms in the vicinity of KMF. The important constraints in sample selection and processing techniques, results and inference are also discussed.

#### **COSMOGENIC RADIONUCLIDES**

The long-lived radioactive nuclides have gained importance in the various streams of science which includes geology, biology, environmental science, medicine, agriculture etc. in the last few decades. In the category of radioactive nuclides, the cosmogenic radionuclides have received increasing application in geology and archeology in the last decades. The advancement in technology and AMS made measurement of these nuclides in earth surface easier. Each paleo-events leaves their signatures in natural archives in the form of radioactive nuclides, therefore the past occurred event can be traced by measuring the radioactive elements (Eisenhaur et al., 1987; Kalish et al., 1994; Von Blanckenburg, 2006; Lupker et al., 2012; Granger et al., 2015). These nuclides are identified extremely useful in dating fault and related landforms (eg. Zreda and Noller 1998; Handwerger et al., 1999; Mitchell et al., 2001; Benedetti et al., 2002; Schlagenhauf et al., 2010; Benedetti et al., 2013; Goodall et al., 2021). The important part of the dating technique is that they provide the timing of faulting activity more precisely than any other dating techniques.

The cosmogenic nuclides are formed in the Earth as a result of nuclear reaction between the cosmic rays and atoms (Lal, 1991). The cosmic rays reaching the earth atmosphere can be broadly classified into Galactic Cosmic Ray (GCR), Solar Cosmic Ray (SCR) and Cosmic rays of anomalous origin (ACR) (Mishev and Velinov, 2007). These high energy cosmogenic rays or primary cosmic rays reaching the earth surface will collide with the element of the earth's atmosphere to produce cascades of low energy secondary cosmic rays. The secondary cosmic rays produced in the atmosphere interact with the target elements to produce number of stable and radioactive cosmic nuclides. The nuclear reaction that results in the generation of cosmic nuclides includes spallation, thermal nuclear capture and low body two body reaction. The production rate of cosmogenic nuclides depends on several factors. Energy of bombarding particle, cosmic ray flux, abundance of target nucleus, location of sample and shielding effect are a few controlling factors of cosmogenic production rate (Lal and Peter, 1967; Jha and Lal, 1982; Lal, 1991).

The cosmogenic nuclides can be classified into two types as in-situ variety and meteoric variety (Lal, 1988,1991; Nagai et al., 2000). Here the meteoric variety includes those produced in the earth's atmosphere whereas, the insitu variant are those produced in the crystal lattice of the minerals in the earth surface. The meteoric variety of beryllium attaches to dust and aerosols in the atmosphere and falls to the earth surface by dry and wet precipitations. More clearly there is a contact shower of meteoric variety of the cosmogenic nuclides to the earth surface. On the other hand, the insitu variety of cosmogenic nuclides are produced in the mineral crystal lattice as a result of interaction of target elements with secondary cosmic rays reaching the earth surface. As a product of this reaction long-lived cosmogenic nuclides are produced in the earth surface and sub-surface to few meters depth. The production rate of the cosmogenic nuclides decreases exponentially below the upper two meters of the surface (Von Blanckenburg and Willenbring, 2014). The atmospheric production rate of cosmogenic nuclides are several times higher than the insitu variety (Lal, 1991). Lal (1991) also envisioned that production rate of cosmogenic nuclides increases with altitude and latitude.

The variety of cosmogenic nuclides are produced in the earth atmosphere based on the target nuclide. Common cosmogenic nuclides are  $^{10}\text{Be}$ ,  $^{26}\text{Al}$ ,  $^{36}\text{Cl}$ ,  $^{14}\text{C}$ ,  $^3\text{He}$  and  $^{21}\text{Ne}$  (Ivy-Ochs and Kober, 2008). In the case of  $^{10}\text{Be}$ , Oxygen and Nitrogen are the best target nuclide in the atmosphere and Oxygen and Silicon as target nuclide for insitu produced  $^{10}\text{Be}$ . The atmospheric average production rate of  $^{10}\text{Be}$  is  $4 \times 10^{-2}$  atoms/cm<sup>2</sup>/sec (Daman and Sonnet,

1991). The insitu production rate of  $^{10}\text{Be}$  is several times lesser than the atmospheric production rate, i.e., 4.3 to 3.7 atoms/g/yr (Granger et al., 2013; Balco et al., 2009). Due to the relatively low concentration of cosmogenic radionuclides in the rocks of the earth surface, the traditional mass spectrometric technique cannot be used to measure the insitu cosmogenic nuclide concentration. Therefore, measuring the concentration of insitu produced  $^{10}\text{Be}$  requires ultra-high sensitive instruments like Accelerator Mass Spectroscopy (AMS) (Granger et al., 2013). Apart from the cosmogenic  $^{10}\text{Be}$ , the rocks on the earth surface also contain trace quantity of Beryllium isotope. However, this variety of Beryllium is made of 100%  $^9\text{Be}$ . The  $^9\text{Be}$  present in the rocks of the earth surface releases through weathering process. The  $^9\text{Be}$  produced by weathering and  $^{10}\text{Be}$  removed from the atmosphere combines and get absorbed to clay or gets chemically precipitated with Fe-Mn oxy hydroxides and form coating over the sedimentary grain (von Blanckenburg, et al., 2012). Therefore, these isotopes have very important application in understanding the past climatic and environmental changes. In spite of the fact that meteoric variant has been popular over the last few decades, it is largely eclipsed by the expansion of the application of insitu  $^{10}\text{Be}$  in the recent years.

The advancement in the AMS over past few decades made it possible to accurately and precisely measure various cosmogenic nuclides. Among the cosmogenic nuclides  $^{10}\text{Be}$ ,  $^{26}\text{Al}$  and  $^{36}\text{Cl}$  are the widely used isotopes in the geomorphic applications. The long-lived isotopes like  $^{10}\text{Be}$  and  $^{26}\text{Al}$  have half-life of  $1.389 \pm 0.014$  Ma and  $0.708 \pm 0.017$  Ma respectively (Korschinek et al., 2010; Nishiizumi, 2004). The long half-life of these isotopes makes it possible in decoding information regarding paleo events up to 10 million years. The 10 million years is very important for geological community as it covers the Quaternary and a large part of Late Tertiary periods. In the present day the cosmogenic nuclide is widely used in different areas of Geology, especially in geomorphology and glaciology (Granger et al., 2013). Cosmogenic  $^{10}\text{Be}$  was also used by several researchers in determining the age of sediment and sedimentation rate of marine sediments (Bourles et al., 1989; Kim and Nam, 2010). Other than this, cosmogenic  $^{10}\text{Be}$  was used by several researchers in qualifying the earth surface processes that includes erosion rate, denudation rate, exposure date etc. (Brown et al., 1992; Mackey et al., 2009; Charreau et al., 2011; Portenga and Bierman, 2011; Von blanckenburg, 2012, 2014). Information regarding the earth surface processes are crucial for understanding the major controlling factors on landscape evolution.

Cosmogenic nuclides are widely used in understanding the geomorphological phenomenon happening on the earth surface. In geomorphology, the radionuclides are used in two different ways. The first application is to ascertain the age of geomorphological event and the second application is for measuring the rate at which landform change occurred through time (Cockburn and Summerfield, 2004). In the dating of faulting and related landform changes have gained importance in the last few decades. The terrestrial cosmogenic radionuclides are used widely in estimating the slip rate and earthquake recurrence intervals. The inferring of fault displacement histories by using cosmogenic nuclide inventories in the bedrock scarps is a widely adopted technique used to comprehend the evolution of fault over the course of time (Goodall et al., 2021). A strong knowledge of fault evolution helps to address the fundamental concerns of how the fault interact with the landscape and how tectonic strain accumulates and release across time and space. The bedrock normal scarps are good target for cosmogenic exposure dating as they preserve a detailed history of fault exposure in comparison to other tectonically displaced landforms (for eg. Benedetti et al., 2002; Schlagenhauf et al., 2010; Cowie et al., 2017; Mechernich et al., 2018; Goodall et al., 2021).

Other important application of cosmogenic nuclide is that these nuclides help in understanding the rate at which rivers incise or erode the rocks. The measurement of cosmogenic nuclide concentration in river worn rock, cave deposit and abandoned strath terraces helps in qualifying the river incision rates (Seidl et al., 1997; Hancock et al., 1998; Granger et al., 1997, 2001; Leland et al., 1998). Hancock et al. (1998) measure  $^{10}\text{Be}$  on sample collected directly from the river bed in understanding the millennium rate of incision. In contrast, Leland et al. (1998) measured  $^{10}\text{Be}$  concentration to establish the incision rate of river Indus in tectonically active Himalayas.

The cosmogenic radionuclides are widely used in the establishing age and exhumation of fault related landform (Gosse and Phillips, 2001; Schlagenhauf et al., 2010; Granger et al., 2013; Tesson et al., 2016; Tesson and Benedetti, 2019; Goodall et al., 2021). However, the application of the nuclides is less used in the Kachchh basin. Situated in tectonically active region in the trailing end of the Indian plate, the basin is characterized by a wide variety of landforms produced by periodic tectonic uplift and erosion. The cosmogenic nuclide and exposure dating technique will be an important tool in establishing the age and rate of development and exhumation of the landform in the basin. The

application of the cosmogenic radionuclides in establishing the age of landscape evolution along the KMF is discussed in the following sections.

### **JARA-JUMARA SECTOR- Western KMF**

The Jara-Jumara sector in the western side of the KMF is characterized by peculiar twin parallel scarps. The development of the scarps and associated gorges requires well constrained chronological studies. In the following sections the geological settings, sample collection strategy for the Jara-Jumara sector is discussed.

#### **Jaramara Scarp**

The Jaramara Scarp as discussed in the previous chapter is a significant landform in the Jara-Jumara sector (Chapter 3). The Jaramara Scarp is formed on rigid sandstone member of upper Jhuran Formation (Fig. 7.1 a). Petrographic and modal point count data for sandstones of Jhuran formation revealed that the average percentage of quartz in the formation is 57% (Chaudhuri et al., 2018). Hence, it is expected that quartz content in the sample collected from the formation can be used for exposure dating as it is present in adequate quantities. The upper Jhuran sandstone is comparatively hard and erosional resistant as compared to the lower Jhuran formation that forms the base of the scarp (alternate layers of sandstone and shale). The quartz rich, extremely hard, erosion resistant sandstone member that makes the Jaramara Scarp thus amenable for cosmogenic isotopic analysis. Considering that the Jhuran formation is Mesozoic in age, it is unlikely that nuclide activity inherited from previous exposure should be negligible. Several lines of evidence indicates that origin of Jaramara Scarp is not resultant of recent surface rupture and retreat. The scarp forms a secondary drainage divide for few north flowing rivers. Considering the presence and size of the rivers it is unlikely that scarp formation occurred in the recent period. Moreover, the bedrock scarp does not consistently coincide with the active fault trace. The present scarp is expected to be the product of long-term tectonically induced erosion along western KMF. Therefore, the exposed lithologies in the scarp top is expected to contain ample concentration levels of  $^{10}\text{Be}$  for isotopic analysis.

#### **Jara River gorge**

The Jara River has a gorge system that is well developed in the upper Jhuran sandstone and Miliolite Formation in the upstream of the Jara River. (Fig. 7.1 b and d). The river drops 60m along the zone of gorge. The gorge is characterized by multiple set of knickpoints. The sandstone exposed at the gorge bottom is the same sandstone member

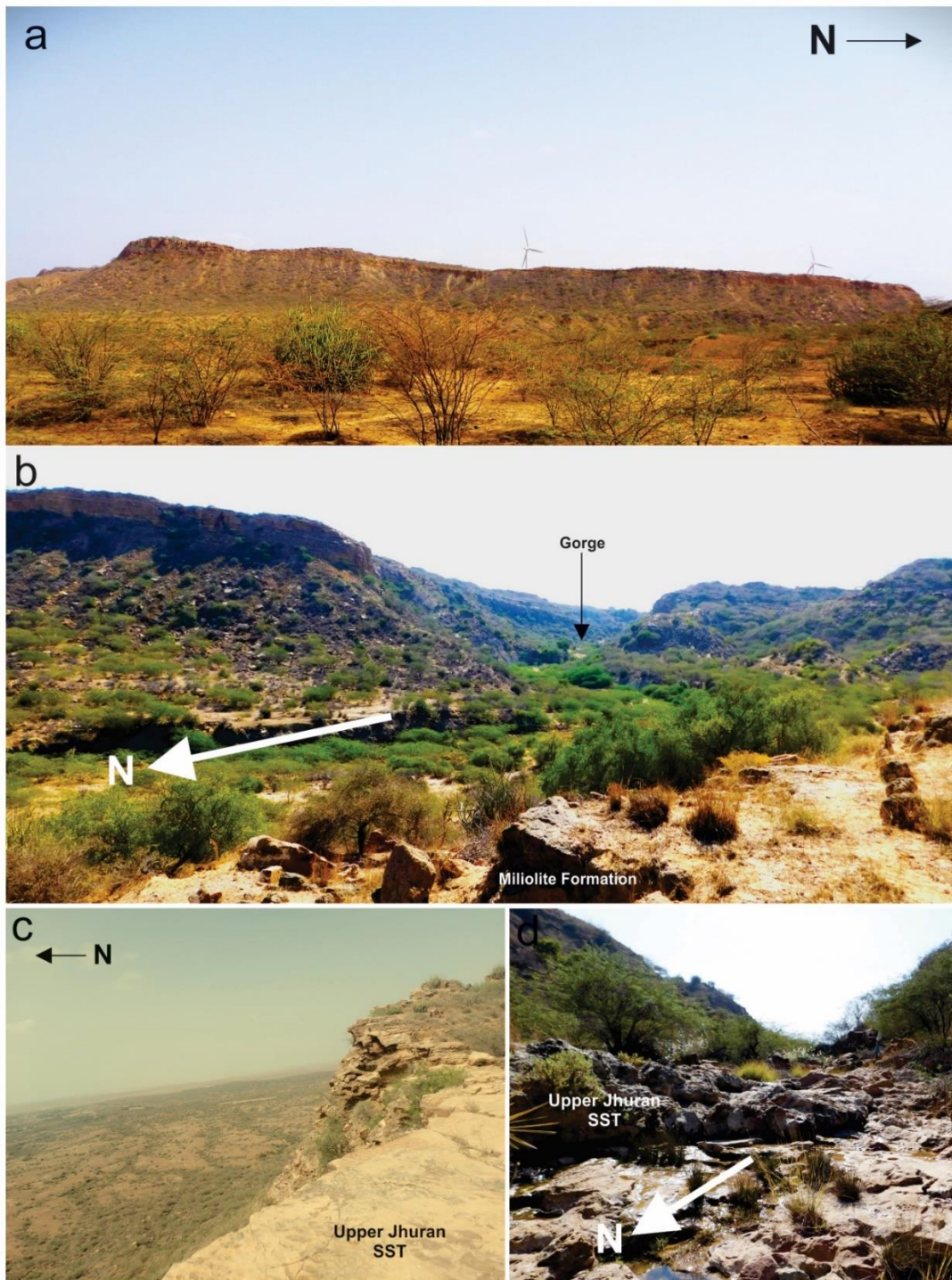


**Figure 7.1** (a) Southward view of the Jaramara Scarp. (b) Photograph showing southward view of Jara River gorge. (c) Field setting of Jaramara Scarp. Note the hard upper member of Jhuran Formation exposed at the summit of the scarp. (d) Field setting of Jara River gorge. The river incises through hard upper member of Jhuran Formation.

exposed at the summit of Jaramara Scarp. Therefore, the exposed lithology should contain sufficient amount of quartz, a target mineral for  $^{10}\text{Be}$  exposure dating. Meanwhile, petrographic analysis of miliolites occurring inland of Kachchh basin indicates that these rocks contain 60-90% bulk quartz grains (Biswas, 1971). The sandstone units that make the

gorge walls is quartz rich thus amenable for cosmogenic isotopic analysis. The magnitude of nuclide activity inherited or memory of  $^{10}\text{Be}$  in previous exposure is expected to be negligible. As mentioned in the previous section, the upper Jhuran formation being of Mesozoic age any inherited  $^{10}\text{Be}$  would have decayed and reset the chronological clock to zero. However, the magnitude of  $^{10}\text{Be}$  inherited from prime period of exposure is unknown in the case of miliolite. The presence of incised miliolite and multiple knickpoints developed in hard sandstone high suggest that the gorge formation occurred in Early Quaternary period. The formation is expected to contain ample quartz contents having measurable concentration of  $^{10}\text{Be}$  for isotopic analysis.

### **Sample collection strategy for Jara-Jumara sector**

For understanding the evolution of the footwall flexure and subsequent gorge development needs a more tactical approach. Taking the geological settings into consideration, the sampling has been limited to Jaramara Scarp summit and the Jara River gorge. Sample from the scarp face was avoided as the Jaramara Scarp face is highly eroded and broken. Moreover, the scarp face appears to be resultant of frequent slope failure and gravity collapse. Therefore, sampling of the scarp face can yield a much younger age because of frequent gravity collapse of the scarp face and exposure of fresh surface. The sample taken from the scarp summit is labeled as JS-1 (Table 7.1). The scarp summit is characterized by less vegetation, near horizontal surface and lack of sedimentary cover. Therefore, the summit of the scarp is the most amenable site for cosmogenic surface exposure dating. The Jara River gorge in the location was sampled from top to bottom (JRG-3, JRG-2, JRG-1). The samples JRG-3 and JRG-2 is from the Miliolite Formation, however JRG-1 is from the hard sandstone member of upper Jhuran Formation. The miliolite limestone that forms the upper part of the gorge helps to have an age control on our studies. The miliolite deposits of Kachchh basin was extensively studied by Baskaran et al. (1989) and Sharma et al. (2017) and established the age of deposition between 130ka -30ka. Therefore, present incision of the river through miliolite deposit should be Late Pleistocene or younger. A chisel was used to collect samples from the vertical surface of the scarp. The latitude, longitude and altitude data for the collected samples were measured at the field.

Utmost care has been taken to avoid areas of the surface that were extensively fractured and eroded. The samples were chiseled from the upper surface of the scarp with thickness 7-10 cm. The thickness of each sample was recorded to reduce the error in the calculation of scaling parameter and the final exposure age. Other parameter required to

calculate the shielding parameters like dip and strike of the sampling surface were measured at the field. Photographs of each site including location of the samples, are shown in the supporting information. Assumed that zero inheritance from previous exposure and minimal influence of climate in the  $^{10}\text{Be}$  concentration in the rocks. The Mesozoic lithologies that make up the scarp summit have deposited during the cretaceous period (Upper Jhuran member) (Fig. 7.1 c). Therefore, any memory of  $^{10}\text{Be}$  produced during the deposition of the formation would have degraded and reset the clock to zero before getting exposed via gorge formation or erosion.

## KAS HILL SECTOR-Eastern KMF

### Khirsara fault scarp

The Kas Hill sector along the eastern KMF is also characterized by twin parallel

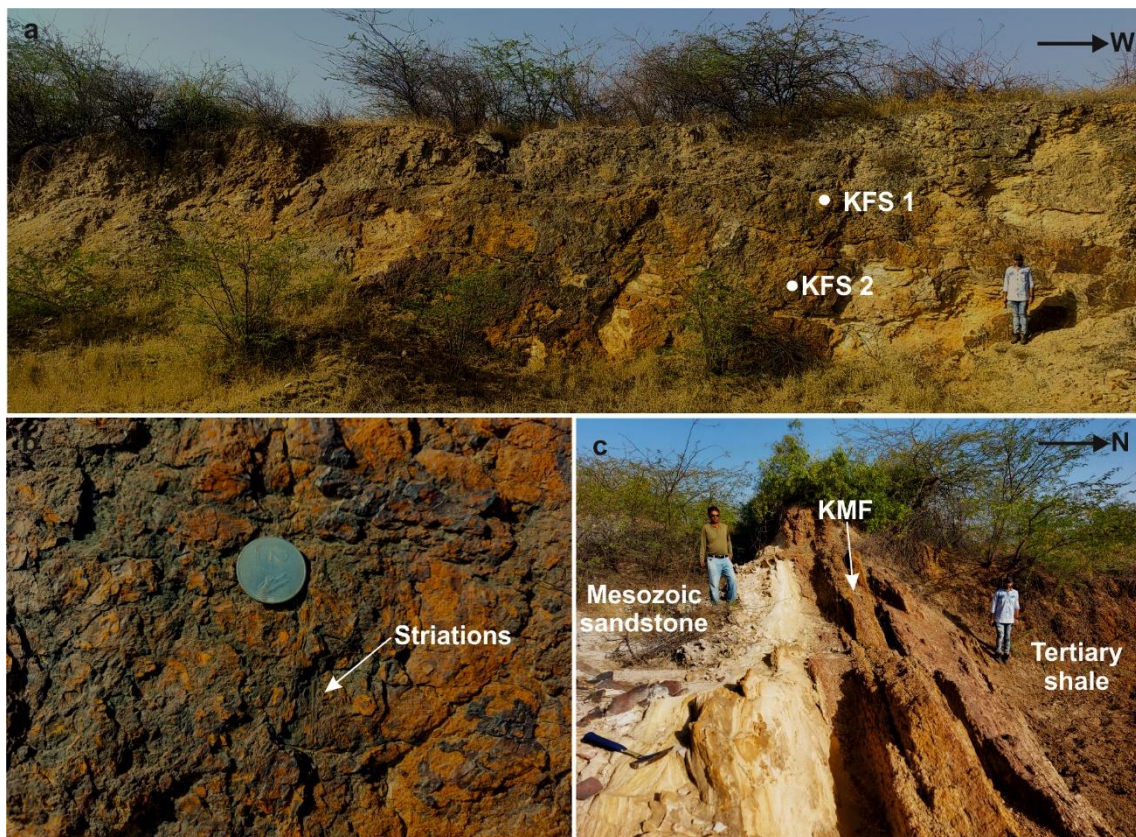


**Figure 7.2** (a) Southward view of the KMFS in the Jhuran anticline near Khirsara village. Note the location of samples collected for cosmogenic surface exposure dating. (b) Close view of fade striations in the scarp. Fade striations are indicating preserved fault plane. This makes the scarp most suitable location for cosmogenic exposure dating. (c) Field setting of KMF as observed in the Khirsara region. The KMF marks the sharp lithotectonic contact between near vertical Mesozoic rocks to the south and Tertiary rocks to the north.

scarp system. In which the Khirsara scarp is located in the eastern most extension of Kas Hill Scarp. Further east, the Kas Hill Scarp becomes undetectable/dies out. The Khirsara scarp is developed in the Bhuj sandstone of upper Cretaceous period (Fig. 7.2 a). The scarp is 6m high and have almost vertical scarp face (slope-85°). The scarp is characterized by faded striations (Fig. 7.2 b). The faded striations visible on the scarp face indicates that scarp face is less affected by weathering and erosional process after formation. Furthermore, the scarp in the location coincides with the actual fault trace. The KMF in the location forms the lithotectonic contact between Bhuj sandstone and Tertiary formation (Fig. 7.2 c). Petrographic and modal point count data for sandstones of Bhuj Formation revealed that the average percentage of quartz is 59% (Chaudhuri et al., 2018). The sandstone that makes the scarp face is quartz rich, extremely hard, erosion resistant thus amenable for cosmogenic isotopic analysis. The magnitude of nuclide activity inherited or memory of <sup>10</sup>Be in previous exposure will be negligible. The Bhuj formation being of Mesozoic age any inherited <sup>10</sup>Be during deposition would have decayed and reset the chronological clock to zero before getting exposed via faulting.

### **Sample collection strategy for Kas Hill sector**

The major fault scarps of KMF are degraded and retreated to some distance from the fault line. Therefore, sampling from these degraded scarp surfaces will not yield the faulting histories or timing of evolution. Moreover, one can expect a much younger age because of frequent gravity collapse in these surfaces. For understanding the evolution of the footwall flexure and subsequent fault scarp development will require a more tactical approach. Here, taking the geological settings into consideration, the sampling is limited to scarp surfaces where the fault planes were well preserved. The geological setting of the Khirsara scarp makes it an excellent location for cosmogenic exposure dating. The scarp in the location was sampled at the top and bottom. A chisel was used to collect samples from the vertical surface of the scarp. The latitude, longitude and altitude measurement for the collected samples was done at the field. Maximum care has been given to avoid areas of fault plane that was extensively fractured and eroded. The samples were chiseled from the upper surface of the scarp with thickness 7-10 cm. The thickness of each sample was recorded to reduce the error in the calculation of scaling parameter and the final exposure age. Other parameters like dip and strike of the sampling surface were recorded in the field. Photographs of each sites including location of the samples are shown in the supporting information. The scarp

ages assume zero inheritance from previous exposure and minimal influence of climate in the  $^{10}\text{Be}$  concentration in the rocks.

### **SAMPLE TREATMENT FOR $^{10}\text{Be}$ DATING**

Chemical preparation for isolation of  $^{10}\text{Be}$  isotopes was done at the National Geochronology Laboratory of Pondicherry University. Standard method described by (Corbett et al., 2016) was followed for sample preparation and chemical processing (Fig. 7.3). The rock samples were initially crushed and powdered manually to separate fraction of 80 -120 $\mu\text{m}$  size range through wet sieving. The particles larger than 80  $\mu\text{m}$  size were re-crushed and powdered again to achieve the desired size range of 80 -120 $\mu\text{m}$ . The size fraction below 120 $\mu\text{m}$  were discarded. Approximately 200g of the sample was taken for magnetic separation using a hand magnet. The sample was then passed through Franz Isodynamic separator to extract pure quartz grains from the sample. Different magnetic fractions were separated using different slope and current. Finally, quartz grains were isolated at a current 1.4 A and a reverse side slope of -5. Samples separated from the isodynamic separator were analysed under a binocular microscope to make sure that the samples were free of impurities. More than one round of isodynamic separation was required for those samples having higher proportion of impurities. Samples were then taken for chemical leaching using a mixture 2% HF and 5 %  $\text{HNO}_3$  to separate the meteoric variant of Be isotope and other contaminants from the sample surface. However, for the sample JRG-2 bromoform separation was performed to separate out quartz from the feldspar grains before chemical leaching. However, the attempt was unsuccessful and the sample was discarded. The other samples were leached 4-5 times to purify the quartz and eliminate atmospheric  $^{10}\text{Be}$ . To get the best results, the mixture of 2% HF and 5%  $\text{HNO}_3$  was renewed in every 24 hours followed by section of ultra-sonication for 15-20 minutes. The leachates from the multiple cycles of chemical leaching were dried and weighed. The samples were digested at a temperature of 120 $^\circ\text{C}$  using concentrated HF. The fluoride complexes formed while digesting were expelled by adding concentrated  $\text{HNO}_3$ . The samples were digested for more than 2 weeks and it was ensured that complete digestion of the sample was attained and the quartz grains were fully dissolved. The digestion was carried out using 250ml PFA beakers and hot plate. In order to lower the risk of contamination, normal glass beakers were avoided for digestion. The digested quartz was made up to 10ml using concentrated HCL and Milli-Q in a centrifuge tube. 1ml of the solution was separated for natural  $^9\text{Be}$  analysis.  $^9\text{Be}$  present in the samples was measured using ICP-MS (X-Series model, Thermofisher Scientific) facility at the

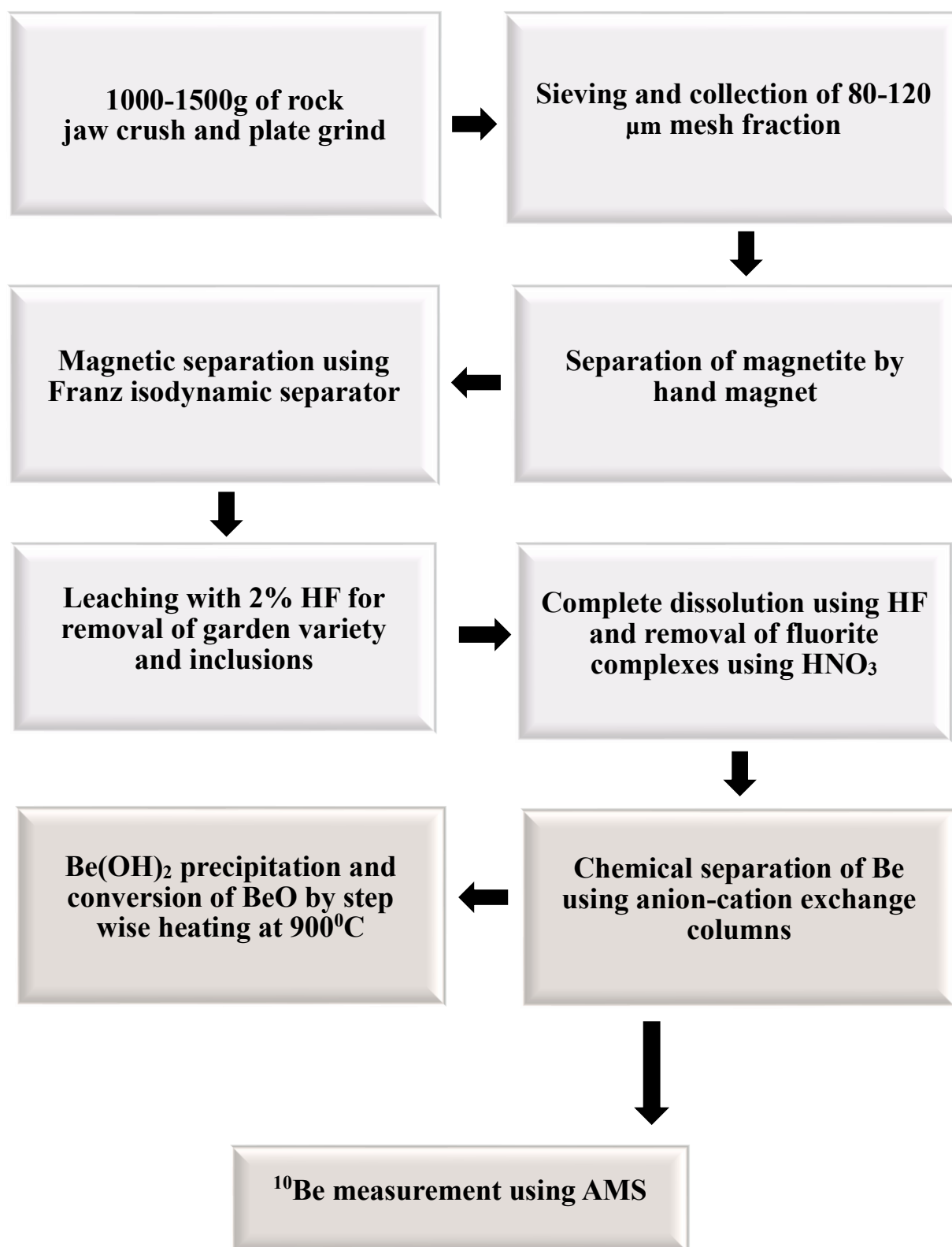


**Figure 7.3** Flow chart depicting the procedures adopted for chemical processing and extraction of  $^{10}\text{Be}$  in the rock samples. The  $^{10}\text{Be}$  concentration obtained from the AMS was used for exposure age estimation for the present study.

Department of Earth Sciences, Pondicherry University. Remaining solution was spiked with approx. 0.1g of  $1005 \pm 5$  ppm  $^9\text{Be}$  carrier solution. The samples were then passed through anion exchange column (Bio-Rad, AG 1 $\times$ 8, 200-400 mesh) and cation (Bio-Rad, AG-MP resin, 200-400 mesh) exchange columns for separating other elements like Iron, Magnesium, Calcium and alkali metals.  $^{10}\text{Be}$  isotope was isolated by cation exchange in a 1.2N HCl solution. The  $\text{Be}(\text{OH})_2$  was precipitated using  $\text{NH}_4\text{OH}$  solution at a pH range of 7-8 in a centrifuge tube. By utilizing both coarse and fine pH indicator strips, the solution was adjusted until it reached the desired pH range. The precipitated  $\text{Be}(\text{OH})_2$  was centrifuged for 15-20 minutes and transferred to Quartz vials. In order to oxidize beryllium hydroxide, a stepwise heating procedure was carried out in a high temperature furnace for more than twenty-four hours at a selected temperature range.  $\text{BeO}$  was mixed with Nb powder and loaded in the cathodes for AMS detection. The  $^{10}\text{Be}/^9\text{Be}$  measurements were carried at Inter-University Accelerator Centre (IUAC), New Delhi using 500 kV XCAMS Accelerator Mass Spectrometer facility. Standard sample NIST SRM 4325 was used for the calibration of the AMS system and the measured results of studied samples were normalized to the standard sample SRM 4325 and background is corrected with blank samples. When analysing the rock samples for cosmogenic nuclide concentration it is important to take topographic shielding factors into consideration (Balco et al., 2008). All the data were organised, formatted and were input into CRONUS- Earth online calculator (version 3.0) for age determination.

## RESULTS

### Khirsara fault scarp

The cosmogenic exposure dating demonstrates that the Khirsara scarp formation occurred in the Late Quaternary period. The model ages for the samples are KFS1 and KFS 2 are  $318 \pm 43\text{ka}$  and  $249 \pm 52\text{ka}$  respectively. The age was calculated taking model proposed by Lal (1991) and Stone, 2000. The scaling factor is generally assigned based-on latitude and altitude scheme of Lal (1991) recast as function of latitude and atmospheric pressure by Stone (2000).  $^{10}\text{Be}$  concentration measured by AMS for KFS-1 and KFS-2 are  $2.2016 \pm 0.2123 \times 10^{-12}$  and  $9.0581 \pm 1.637 \times 10^{-13}$  respectively. At the site, the  $^{10}\text{Be}$  concentration increases gradually with increasing height. This is because the top of the scarp (sample KFS 1) is exposed for longer period of time, albeit the difference is not significant (Table 7.1). Considering the geological setting and ages obtained from the cosmogenic nuclide analysis

it is confirmed that a major scarp forming event occurred along KMF during the Mid Pleistocene period.

### **Jaramara Scarp**

The model exposure age for the sample JS 1 is  $102 \pm 15$ ka. The age was calculated taking into consideration of the model proposed by Lal (1991) and Stone (2000). The age was calculated similar to procedure explained above (Lal, 1991 and Stone, 2000).  $^{10}\text{Be}$  concentration measured by AMS for JS 1 is  $1.6196 \pm 0.1970 \times 10^{-12}$ . At the site, the  $^{10}\text{Be}$  concentration in the sample is comparatively less. Generally, the scarp summit should yield higher concentration of the  $^{10}\text{Be}$  because of higher elevation and lower erosion at the summit. Additionally, on a horizontal surface,  $^{10}\text{Be}$  is produced at a rate that is several orders of magnitude higher. However, compared to samples from the Khirsara scarp, which is at a considerably lower elevation and samples were obtained from the vertical scarp face, the  $^{10}\text{Be}$  concentration in the current instance is somewhat lower (Table 7.1). The considering the ages obtained from the cosmogenic nuclide analysis it is revealed that the present surface of the Jaramara Scarp got exposed to cosmogenic rays during Early-Late Pleistocene period.

### **Jara River gorge**

According to the cosmogenic exposure ages obtained from the Jara River gorge, the samples the JRG 1 and JRG 3 gave an age of  $1003 \pm 151$ ka and  $268 \pm 37$ ka of age respectively.  $^{10}\text{Be}$  concentration measured by AMS for JRG-1 and JRG -3 were  $3.9279 \pm 0.3355 \times 10^{-12}$  and  $2.3932 \pm 0.2487 \times 10^{-12}$  respectively. The concentration of  $^{10}\text{Be}$  in the sample is JRG-1 was very high in comparison with the other samples. Generally, in a vertical surface one should expect relatively lower concentration of the  $^{10}\text{Be}$  because of higher shielding factor and lower production rate. However, in the present case the  $^{10}\text{Be}$  concentration is very high and is in an order of  $10^6$  (Table 7.1). The ages calculated from the JRG-1 suggest that present surface gorge wall at the location of JRG-1 got exposed in the Early Pleistocene period. Considering the location of the sample JRG-1 inside the Jara River gorge, it is possible to get to the conclusion that the incision and gorge formation commenced much earlier than the exposure age obtained from JRG-1. The cosmogenic age obtained from the miliolite (JRG 1) at top of the gorge is  $268 \pm 37$ ka (Table 7.1). With respect to the time period for miliolite deposition in the Kachchh basin, 130ka to 30ka, the age obtained from cosmogenic analysis for the present sample is overestimated.

**Table 7.1**  $^{10}\text{Be}$  inferred surface exposure ages.  $^{10}\text{Be}/^9\text{Be}$  ratios were blank and spike corrected.

Sample	Quantity (g)	Latitude	Longitude	Alt. (amsl)	Shielding Factor	$^{10}\text{Be}/^9\text{Be}$ ratio in the order $10^{-10}$	$^{10}\text{Be}$ conc. (atoms/g)	Exposure Age (ka)
<b>Khirsara scarp-Eastern KMF</b>								
KFS 1 (Scarp Top)	29.50816	23°20'52.10"N	70° 3'23.30"E	35m	0.500066	$1.75 \pm 0.169$	$(4.89 \pm 0.47) \times 10^5$	318 $\pm$ 43
KFS 2 (Scarp Bottom)	15.72458	23°20'52.10"N	70° 3'23.30"E	33m	0.500066	$1.62 \pm 0.293$	$(3.89 \pm 0.74) \times 10^5$	249 $\pm$ 52
<b>Jumara scarp summit and Jara River gorge-Western KMF</b>								
JS 1	30.6327	23°41'42.00"N	69° 0'55.40"E	147	0	$2.70 \pm 0.328$	$(3.55 \pm 0.43) \times 10^5$	102 $\pm$ 15
JRG-1	19.26459	23°41'21.30"N	69° 0'15.40"E	84	0.501008	$6.4 \pm 0.547$	$(1.37 \pm 0.12) \times 10^6$	1003 $\pm$ 15
JRG-3	18.9323	23°41'21.30"N	69° 0'15.40"E	87	0.501008	$2.82 \pm 0.293$	$(8.51 \pm 0.88) \times 10^5$	268 $\pm$ 37

The higher concentration of  $^{10}\text{Be}$  in the sample could be attributed to the inherent  $^{10}\text{Be}$  with the sample before getting exposed via gorge formation. The miliolite being of aeolian origin and the quartz grains within the formation were transported from inland areas to present location by the action of wind. The grains would have been in constant exposure to cosmic rays before deposited to the present location. The exposure to cosmic rays would result in the production of  $^{10}\text{Be}$  in the sample. The  $^{10}\text{Be}$  being a long-lived radio nuclide (half-life- 1.39Ma) it requires minimum 1.38Ma to decay and reset the chronological clock to zero (Korschinek et al., 2010). The presence of inherent or memory of previous exposure in the quartz mineral resulted in an over estimation of the age. The sample JRG-3 is not used in the interpretation of present study.

## **IMPLICATION OF SURFACE EXPOSURE CHRONOLOGY**

### **Khirsara fault scarp**

Two prominent exposure ages were obtained for the Khirsara scarp. The ages indicate the Mid Pleistocene reactivation of the KMF. The exposure ages indicate the youngest scarp forming event occurred along the KMF during the Mid Pleistocene period. The ages obtained from the cosmogenic exposure ages are in good agreement with the progressive decrease in the scarp height, reduction in the thickness of colluvio-fluvial deposits and diminution in the grain size of sedimentary facies towards eastern KMF. The current age derived from the exposure dating of the scarp also suggests that a major paleo earthquake occurred along the KMF during the Mid Pleistocene period. However, to calculate the magnitude of the earthquake and slip rates requires more exposure ages. The KRB has gone through several episodes of tectonic uplift and erosion ever since the Late Cretaceous period (Biswas, 1993). Among the events, the tectonic disturbances occurred during the Early Quaternary was one of the notable phases of tectonic uplift and erosion. Biswas (1993) also envisioned that towards the later part of the Pliocene and Pleistocene, the sedimentation was predominantly continental and it was accompanied by tectonic uplift and erosion. Our ages are in good agreement with the tectonic uplift that occurred in the Pleistocene period. Considering the general trend of the basin it can be concluded that the Mid Pleistocene heightened tectonic uplift was accompanied by an elevated phase of landscape erosion along the KMF. The elevated phase of erosion could result in the higher rate of degradation of landforms in the vicinity of the KMF. The exposure ages also indicate a lateral propagation of the KMF towards the eastern side during the Mid Pleistocene period. The progressive decrease in the scarp height and the height of Northern

Hill Range Flexure Zone (NHRFZ), reduction in the thickness of the colluvio-fluvial deposits, decrease in the degree of dissection by the fluvial channels and diminution of the sedimentary facies grain size further corroborate the finding of the lateral propagation of the KMF during the Quaternary period.

### **Jaramara Scarp**

The Jaramara Scarp is a prominent landform located several kilometers south of the present KMF. The sample collected from the summit of the scarp shows an exposure age of Late Pleistocene, i.e.,  $100 \pm 2$  ka. Climate and tectonics are the two-forcing mechanism for erosion of a landscape (Parker and Perg, 2005). The sample collected from the summit of the Jaramara Scarp had more recent exposure ages. There are two possibilities for the cosmogenic derived recent exposure ages. First, the climate led to more effective erosional processes, therefore resulting in younger exposure ages. However, the modern climate of the study area is arid to semi-arid and receives an average rainfall of 30cm/year. The aeolian miliolite deposits in the region also indicate arid to semiarid condition that have prevailed during the Mid to Late Pleistocene period. Second possibility of recent exposure age is higher tectonically induced erosion during the Late Pleistocene period. Burbank et al. (1996) in the coupled tectono-geomorphic model postulated that high strain rate in a topography is directly related to high erosion rate. The higher erosion rate of the landscape led to the exposure of the present surface at the summit of the Jaramara Scarp. Cosmogenic nuclide concentration on a surface decrease with decrease in the length of exposure at a surface due to higher erosion rate (Philip et al., 2003; Ivy-Ochs and Kober, 2008). However, studies on the cosmogenic dating of escarpment confirms that summit denudation is several times lesser when compared to the escarpment face (for eg., Vanacker et al., 2007). This is because the vertical face of the scarp is more prone to uplift induced gravitational driven scarp collapse result in the exposure of fresh surface which attribute a much younger cosmogenic exposure age. However, the summit of the scarp being more stable erodes or undergoes denudation at a much slower rate (Vanacker et al., 2007).

The rate of degradation of scarp depends on the rate at which the surface process act at the slope face. Presence of more factures, broken rocks, area of weakness and faults can lead to higher rate of degradation of the scarp face (Wallace, 1977; Nash, 1980). In the present study area at the vicinity of Jaramara Scarp there are few cross faults and joint set. The presence of these minor secondary faults and joints must have augmented the rate of scarp degradation. At the same time, the field investigation of the present study reiterates

that a major fault other than KMF, which can influence the scarp formation and degradation is absent in the vicinity of Jaramara Scarp. Therefore, the evolution and modification of the Jaramara Scarp is directly influenced by the tectonic movements along KMF. The scarp degradation after formation occurs through cycles or stages (Leeder and Jackson, 1993). In the model (Leeder and Jackson, 1993) proposed that initial stages of scarp degradation will be dominated by gravity spalling from the face and accumulation at the scarp base. This process is succeeded by decline in slope angle and formation of gullies and drainage networks. As time passes, prominent the drainage networks will develop in the scarp and form a central drainage divide. Taking the various stages of scarp formation into consideration the Jaramara Scarp is in the relatively mature stage where the scarp forms a secondary drainage divide in the region. The profiles drawn across the slopes can be used to understand the major geomorphic controlling factor (Ritter et al., 2011). The profiles drawn across the Jaramara Scarp are concave in shape. The concave shape of the scarp and drainage analysis from the present work indicates that erosional process is dominant in the scarp surface (Wallace, 1977; Nash 1980). The Jaramara Scarp base is dominated by boulders and debris derived from the scarp face. The concave shape of the scarp along with debris and boulders deposited at the scarp base points to the fact that the scarp is retreating and migrating backward. The younger exposure ages are because of the faster exhumation as a result of tectonically induced geomorphic processes. Colluvio-fluvial deposits at the base of KMF scarp and KMF zone in the eastern Kachchh suggest the occurrence of three major events during the Late Pleistocene (Maurya et al., 2017). The oldest event occurred during 100ka suggesting a major phase of tectonic uplift and erosion along the KMF zone during that time. The exposure age from the Jaramara Scarp summit is in agreement with the oldest tectonic event reported along the eastern KMF. This suggests that the tectonic event occurred all along the KMF, however amplitude of the movement was very less in the western KMF. The comparatively lesser thickness of colluvio-fluvial or concealed colluvio-fluvial deposit confirms the finding.

## **CONCEPTUAL MODEL FOR JARA RIVER GORGE EVOLUTION**

The long-term studies concerning fluvial landforms, deposits and their response to external controls can play an important role in understanding the dynamic interaction between tectonics and surface processes (Blum and Tornqvist, 2000). In which, bedrock gorges are spectacular landforms that are produced as a result of intense fluvial downcutting or erosion. In river hydraulics, gorge formation begins when, the sediment transport capacity

surpasses the sediment production in a region over a long-term period (Howard et al., 1994). Critical parameters including lithology, climate and tectonics govern gorge development across landscapes. Therefore, investigating bedrock gorges will infer details on past land level fluctuations, climate change and tectonics (Whipple et al., 2000). The thorough understanding on tectonics and surface processes helps in establishing a landscape evolutionary model with less discrepancies. River downcutting into the underlying rock is characteristics of erosional dominance in the landscape (Gupta et al., 2007). The coupled tectono-geomorphic model suggest that high strain rates are spatially associated with high erosional rates (Burbank et al., 1996). The Kachchh Mainland is characterized by several bedrock gorges, which contrast with the present arid climate. The Jara River gorge is one such spectacular landform in the western KMF, that dissects the Jaramara Scarp. Important revelation on gorge formation in the region will shed light on the evolution and degradation of Jaramara Scarp in the footwall of the KMF. Cosmogenic exposure age suggests that incision and sculpting of the landscape commenced even before 1Ma years BP. The rivers flowing through the Jara-Jumara sector of western KMF is strongly influenced by history of vertical movements along KMF (Padmalal et al., 2021; Shaikh et al., 2019). The rivers in the terrain are undergoing effective fluvial erosion into the landscape to adjust with the tectonic pulses occurred in the Late Quaternary period. Other than tectonic influence the region is secondarily influenced by structural control and also lithological control. The long profile morphology of the rivers demonstrates the lithological influence over the river channel other than tectonic influence.

Cosmogenic exposure ages of the rocks exposed in the walls of the valley are essential as it gives crucial information on the phases of incision and tectonic uplift in the region. However, two of the three samples from the top and middle portion of the gorge failed or gave overestimated date. The sample collected from the top portion of the gorge had a fair concentration of Quartz mineral and  $^{10}\text{Be}$  nuclide. However, the age estimated from the sample is 268ka, which is significantly higher than the true age. The miliolite deposition on the highlands and depressions of the Kachchh basin occurred in a time span between 130-30ka (Baskaran et al., 1989). Given the present geological settings of the gorge, it can clear that the incision in miliolite occurred post deposition. Therefore, the ages from the  $^{10}\text{Be}$  exposure dating are the overestimation of the original ages. The higher  $^{10}\text{Be}$  in the samples could be because of the inheritance from the previous exposure. The petrographic and provenance studies on the miliolites of the Kachchh suggest that rock consists of high proportion of wind driven quartz from the inland areas of the basin (Biswas,

1971). The mineral quartz must have been exposed to cosmogenic rays and started producing  $^{10}\text{Be}$  before being deposited in its current location by aeolian activity. Therefore, the age estimated from the top sample was discarded as it can bias the conceptual landscape evolutionary model for the region. The sample collected from the middle portion of the gorge could not be processed because the quartz had too many impurities and also the sample was having higher proportion of feldspar grains. The higher concentration of the impurities and feldspar grains could overestimate or underestimate the original age. However, JRG 1 provided reasonable concentration of  $^{10}\text{Be}$  isotope. The exposure age of sample JRG 1 is at least 1Ma. The present sample location is 19m from the gorge top. More specifically, the river incised more than half portion of the gorge before 1Ma or Early Pleistocene. Details of the stages of gorge evolution in the Jumara sector of western Kachchh are discussed below

#### **i) Stage 1-Initiation of gorge formation**

The cosmogenic exposure age from sample JRG-1 indicates that the Jara gorge formation and channel incision of the river initiated prior to the Pleistocene period (Fig. 7.4 a). The incision of rivers originating from the NHRFZ is attributed to tectonic activity along the KMF (Shaikh et al., 2019; Padmalal et al., 2021). The river shows characteristics of an antecedent river, when one consider the present geological setting of the Jara River into consideration. Since the upper portion of gorge is blanketed by miliolite, it is difficult to assign a definite age for the gorge formation. However, based on the present exposure age from the sample collected from the left bank of the river, the channel incision and gorge formation took place before Pleistocene. The tectonic uplift along the KMF has an important role in the gorge formation, however supported by climatic conditions. The Kachchh basin have gone through several episodes of tectonic uplift and erosion from the Late Cretaceous period (Biswas, 1993). Paleocene, post-Paleocene and post-Miocene are the major phases of reactivation in the Kachchh basin that have resultant in the regional uplift of the basin (Biswas, 1993). Biswas (1993) also proposed that in the later part of the Pliocene to Pleistocene time the sedimentation within the basin was essentially continental as a result of wide spread uplift and erosion. Considering the Pliocene to Pleistocene tectonic disturbances and the cosmogenic ages from the present work, it could be proposed that the bedrock gorge development along the western KMF initiated during the later part of Pliocene. However, continued tectonic uplift to the Early Pleistocene period resulted in further deepening of the valley and exposure of the sample JRG-1 (Fig. 7.4 b). The tectonic

disturbance in the region leads to steep river gradients as result of baselevel changes in the drainage system and simultaneously higher erosion or incision to cope with the disturbances. This indicates that the KMF was active during the Early Pleistocene period. The changes in the river erosional pattern can directly influence the regional denudation rate and hillslope processes.

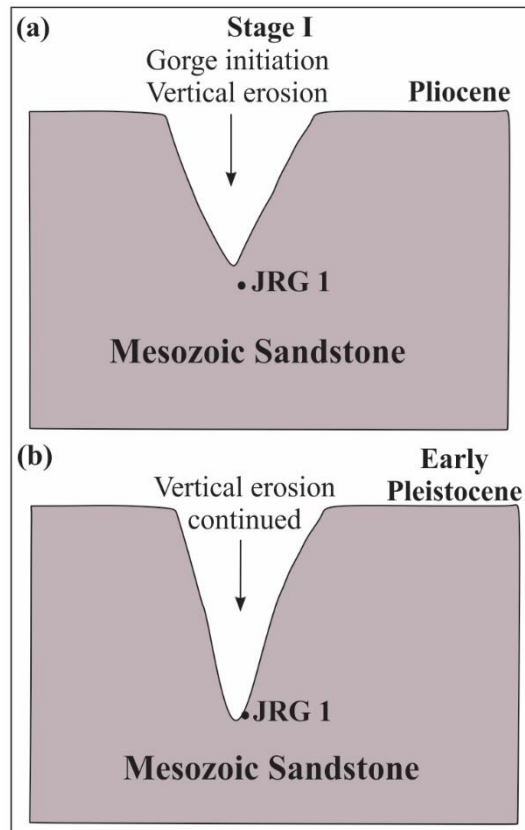


**Figure 7.4** Stages of incision of Jara River and gorge formation. (a) intense incision of the valley during the later part of Pliocene. The sample was not exposed to cosmic rays during the period. (b) the continued tectonic uplift and incision led to further deepening of the channel. The sample got exposed to cosmic rays and started production of cosmogenic  $^{10}\text{Be}$  nuclides.

## ii) Stage 2-Valley widening

Channel morphology with terrace-like platform above the sample JRG-1 suggest that river have broadened the valley after intense vertical incision in the Late Pliocene and Early Pleistocene period. Lateral erosion of the channel can result is valley widening and strath terrace formation. The channel broadening or lateral widening are generally associated to period of mild tectonic uplift (Fig. 7.5 a). This indicates that the region has gone through relatively less tectonic uplift or period of tectonic dormancy during the later part of Early

Pleistocene to Mid Pleistocene. The tectonic dormancy in the region could be directly related to comparatively less or mild tectonic movement along KMF during later part of Early Pleistocene to Mid Pleistocene period.

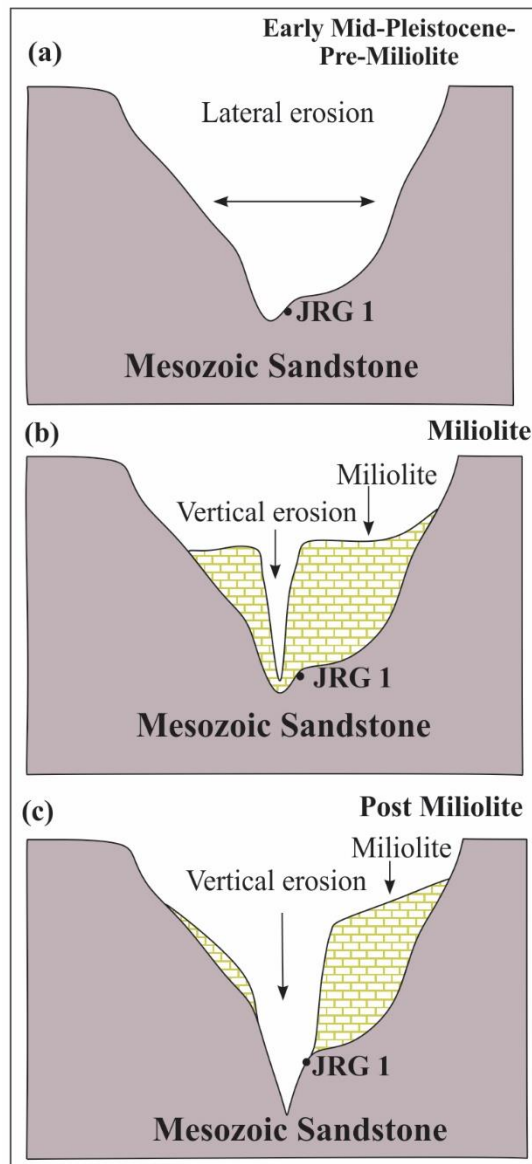


**Figure 7.5** Later stages of gorge evolution. (a) Period of tectonic dormancy in the region led to valley widening and formation of the terrace like platform in the river valley. The sample was constantly exposed to cosmic rays. (b) Infilling of the valley as a result of intense aeolian activity in the Mid Pleistocene period. The sample got buried under the thick aeolian cover for a short period of time. The burial must have inhibited the production of  $^{10}\text{Be}$  in the sample. (c) The Late Pleistocene tectonic uplift that continued to the present led to intense vertical erosion and deepening of the gorge to the present level.

### iii) Stage 3-gorge infilling

The occurrence of miliolite deposits on the left and right bank of the river suggest that intense infilling of the gorge by miliolite happened. The miliolite deposits suggest a phase

of extensive aeolian activity in the region (Fig. 7.5 b). Similar deposition of miliolite and blockage of the river valley is reported from other parts of Kachchh as well (for eg. Maurya et al., 2021). The depositional age of Kachchh miliolite is 130-30ka (Baskaran et al., 1989). The miliolite deposits have partially or fully covered the river valley. The channel was incising through the miliolite deposits. The miliolite being less resistant, the incision rate within the miliolite will be many times higher than the hard upper Jhuran formation. The river requires less power to incise down into the miliolite deposits. The exposure ages obtained from the eastern part of KMF suggest that heightened tectonic activity occurred along the KMF during Mid Pleistocene. The Mid Pleistocene tectonic high and resultant baselevel change resulted incision in the Jara River.

#### **iv) Stage 4-youngest phase of gorge incision**

The tectonic activity occurred during syn and post-miliolite phase results in further vertical erosion into the landscape and deepening of the gorge in the Late Pleistocene period or post miliolite phase. The incised miliolite cliffs downstream of the river and points to the Late Pleistocene tectonic activation of the KMF in the location (Shaikh et al., 2022). The Late Pleistocene channel incision could be directly related to the steepening of channel slopes due to rock uplift. It has been demonstrated that channel gradients dominate hydrological conditions and results in intense bedrock erosion and coarse sediment transport (Kale, 2003). The river incised 6m down to the present bed level in the Late Pleistocene time period (Fig. 7.5 c). This indicate the post miliolite tectonic reactivation of the KMF. The post-miliolite reactivation of other faults is reported in the basin. For example, the post-miliolite reactivation of the KHF led to the deformation of the miliolite deposit and resulted in the vertical dip of the formation. Field studies carried out as a part of the present investigation along the eastern part of KMF identified similar post miliolite reactivation and deformation of miliolite along the KMF. However, the western Kachchh have gone through high sedimentation, resulted in the burial of faultline. The geophysical investigation using GPR has demonstrated the offsetting of the colluvial fluvial and Holocene sediments along the KMF (Shaikh et al., 2022). The above evidences collectively indicate that region has underwent multiple phases of tectonic uplift and erosion during the post-miliolite or Late Pleistocene period. The uplifts and erosion led to further downcutting and erosion of the landscape.

In short, it can be concluded that cosmogenic exposure dating is a useful geomorphic tool for calculating the age of landforms. The lithology and landforms in Kachchh basin are

suitable for cosmogenic exposure dating. For the present study to understand the development of the scarps along the KMF, the undegraded or less eroded scarp was selected for cosmogenic exposure dating. Also, selected landforms near the vicinity of the scarp were chosen for exposure dating to understand their mode of development and link them with the phases of tectonic reactivation along the KMF. The Khirsara scarp is a bedrock rock scarp along the eastern most KMF. The geological setting and lithology were an ideal spot for cosmogenic exposure dating. The exposure ages estimated from the scarp face suggest that a major tectonic event occurred in the eastern part of the KMF during the Late Quaternary period, more precisely during the Mid Pleistocene period. The elevated tectonic uplift along the KMF during the Mid Pleistocene period led to the development scarp along the eastern KMF. The younger age obtained from the scarp confirms the lateral propagation of the KMF during the Mid Pleistocene period. The lateral propagation of the KMF further supported by the decrease in scarp height and degree of dissection by the fluvial channels. The progressive decrease in the thickness of the colluvium and grain size of the sedimentary facies also supports the finding. The degraded scarp surface is not an ideal spot for cosmogenic exposure dating, however, the landforms associated with them can be dated to understand the relative time period of development and degradation. The Jara gorge associated with the Jaramara Scarp is one such landform that helps in the understanding the Late Quaternary phases of reactivation and landform erosion. The miliolite along the Kachchh basin are not ideal lithology for cosmogenic exposure dating without prior petrographic analysis. The rock varies highly in its composition and quartz proportion even with in the Kachchh basin. The higher proportion of feldspar, impurities and inherited  $^{10}\text{Be}$  in the miliolite deposits makes it not an ideal target lithology for exposure dating. The exposure age from the Mesozoic sandstone exposed in the Jara River gorge suggest that the gorge formation commenced in the later part of Pliocene. The exposure age also confirms the tectonic reactivation and uplift induced erosion during the Late Pliocene and Early Pleistocene period along NHRFZ. The continued phases of reactivation of the KMF during the later part of Pleistocene and Holocene resulted in the tectonically induced erosion and deepening of the gorge in the region. Overall, it can be summarized in all possibility that the KMF was active during the Quaternary period.